Received: 8 September 2022 | Revised: 24 November 2022 | Accepted: 27 November 2022

DOI: 10.1002/jex2.69

RESEARCH ARTICLE

Contamination of bacterial extracellular vesicles (bEVs) in human urinary extracellular vesicles (uEVs) samples and their effects on uEVs study

Chadanat Noonin | **Paleerath Peerapen** | **Visith Thongboonkerd**

Medical Proteomics Unit, Office for Research and Development, Faculty of Medicine Siriraj Hospital, Mahidol University, Bangkok, Thailand

Correspondence
Prof. Visith Thongboonkerd, Head of Medical Proteomics Unit, Office for Research and Development, Siriraj Hospital, Mahidol University, 6th Floor – SiMR Building, 2 Wanglang Road, Bangkoknoi, Bangkok 10700, Thailand.
Email: thongboonkerd@dr.com (or) vthongbo@yahoo.com

Funding information
Mahidol University

Abstract

Bacterial overgrowth is common for improperly stored urine. However, its effects on human urinary extracellular vesicles (uEVs) study had not been previously examined nor documented. This study investigated the presence of bacterial EVs (bEVs) contaminated in uEVs samples and their effects on uEVs study. Nanoscale uEVs were isolated from normal human urine immediately after collection (0-h) or after 25°C-storage with/without preservative (10 mM NaN_3) for up to 24-h. Turbidity, bacterial count and total uEVs proteins abnormally increased in the 8-h and 24-h-stored urine without NaN_3. NanoLC-ESI-LTQ-Orbitrap MS/MS identified 6–13 bacterial proteins in these contaminated uEVs samples. PCR also detected bacterial DNAs in these contaminated uEVs samples. Besides, uEVs derived from 8-h and 24-h urine without NaN_3 induced macrophage activation (CD11b and phagocytosis) and secretion of cytokines (IFN-α, IL-8, and TGF-β) from macrophages and renal cells (HEK-293, HK-2, and MDCK). All of these effects induced by bacterial contamination were partially/completely prevented by NaN_3. Interestingly, macrophage activation and cytokine secretion were also induced by bEVs purified from *Escherichia coli*. This study clearly shows evidence of bEVs contamination and their effects on human uEVs study when the urine samples were inappropriately stored, whereas NaN_3 can partially/completely prevent such effects from the contaminated bEVs.

KEYWORDS
bacterial overgrowth, cytokines, exosomes, lipoprotein, macrophage activation, outer membrane vesicles, preservative, sodium azide, urine

1 | INTRODUCTION

Exosomes are the nanoscale membrane-bound extracellular vesicles (EVs) with diameters of 40–160 nm (Jeppesen et al., 2019; Kalluri & LeBleu, 2020). They are found in various body fluids, for example, plasma, urine and saliva (Kumar et al., 2021). Exosomes and other types of EVs, are known to carry several cellular molecules such as proteins, DNAs, RNAs, metabolites, etc. (Jeppesen et al., 2019; Lian et al., 2017; Tao et al., 2019). The presence and abundance of these molecules in exosomes and EVs vary among cell types under different conditions (Chirackal et al., 2019; Jeppesen et al., 2019; Lian et al., 2017; Singhto & Thongboonkerd, 2018; Singhto et al., 2018). In other words, exosomes and EVs isolated from healthy and unhealthy individuals may contain differential levels of proteins (Kerr et al., 2018; Tian et al., 2021), DNAs (Hagey et al., 2021; Zhao et al., 2021), RNAs (Tan et al., 2021; Zhang et al., 2022), and metabolites (Tao et al., 2019; Weingrill et al., 2021; Zhu et al., 2021). Among the body fluid EVs,

This is an open access article under the terms of the Creative Commons Attribution-NonCommercial-NoDerivs License, which permits use and distribution in any medium, provided the original work is properly cited, the use is non-commercial and no modifications or adaptations are made.
© 2022 The Authors. *Journal of Extracellular Biology* published by Wiley Periodicals, LLC on behalf of the International Society for Extracellular Vesicles.

urinary exosomes and other small EVs (*altogether termed as "nanoscale uEVs"*) have gained a wide attention from researchers due to their availability and non-invasiveness of the sample collection (Vitorino et al., 2021). Furthermore, nanoscale uEVs carry various molecules that can be used as the biomarkers for many diseases (Vitorino et al., 2021).

The nanoscale EVs also serve as the cargos for transporting molecules from one cell to the others for their communications. The transported molecules then elicit various effects on the recipient cells (Kalluri & LeBleu, 2020; Lee et al., 2019; Noonin & Thongboonkerd, 2021). As such, the nanoscale EVs have been proposed to be an excellent therapeutic tool to deliver drugs to the target cells *in vivo* (Hazrati et al., 2022; Kalluri & LeBleu, 2020). Although these nanoscale EVs can be used as a drug delivery tool, their sufficient production for therapeutics is quite challenging. Currently, the therapeutic nanoscale EVs are mostly produced from conditioned medium of stem cells, for which procedures are rate-limiting steps, suggesting that large-scale cell culture is required (Colao et al., 2018; Park, 2022). Hence, urine has been suggested to be an alternative source for production of the therapeutic nanoscale EVs. A recent study has shown that the nanoscale uEVs from patients with prostate cancer can be used to deliver nanoparticles containing anti-cancer drug to the cancer cells, *in vivo* and *in vitro* (Pan et al., 2021). More recently, the nanoscale uEVs isolated from premature infant urine has been shown to deliver miR-30a-5p, which is the most abundant miRNA in these uEVs, to the kidney and ameliorate inflammation in mice with acute kidney injury (Ma et al., 2022).

One of the critical issues that should be concerned, when collecting and preparing urine samples for uEVs isolation, is bacterial contamination. It has been clearly shown that bacterial overgrowth can be detected in the urine samples stored at room temperature without preservatives for 8 h (for uncentrifuged urine) and 12 h (for clarified urine after centrifugation to remove cells and debris) (Thongboonkerd & Saetun, 2007). Moreover, such bacterial contamination dramatically affects proteomic analysis of the whole urinary proteome (Thongboonkerd & Saetun, 2007). The overgrowth bacteria can produce and release bacterial extracellular vesicles (bEVs) into the culture medium and the collected body fluids (Bitto et al., 2017; Tulkens et al., 2020). Sizes of bEVs are around 50–250 nm, which overlap with the sizes of human nanoscale uEVs (Hu et al., 2020; Tulkens et al., 2020). Such size overlapping suggests that bEVs are likely to be co-isolated with human nanoscale uEVs if there is bacterial overgrowth in the urine samples. Similar to the human uEVs, bEVs contain components, such as proteins, DNAs, RNAs, etc., from bacteria (Bitto et al., 2017; Bitto et al., 2021; Hu et al., 2020). Hence, the contamination of bEVs in uEVs samples may lead to inaccurate quantification of uEVs contents and may interfere with further uEVs investigations and applications. Nevertheless, their effects on human uEVs analysis had not been previously investigated nor documented.

Recently, the Urine Task Force of the International Society for Extracellular Vesicles (ISEV) has launched a position paper summarizing the state of the art of current research on uEVs (Erdbrugger et al., 2021). One of the challenges and gaps in future uEVs research stated in this position paper by the Rigor and Standardization Subcommittee of the ISEV Urine Task Force is that "*Studies addressing collection, processing and storage of urine specifically for uEVs research are very limited*" (Erdbrugger et al., 2021). Hence, this study aimed to provide direct evidence of bEVs contamination in nanoscale uEVs samples isolated from improperly stored human urine (i.e., that stored at room temperature without preservatives for a long period) and their effects on expression and functional investigations of the uEVs.

2 | MATERIALS AND METHODS

2.1 | Urine sample collection and preparation

All experiments involving human subjects and clinical samples were conducted according to the international guidelines, that is the Declaration of Helsinki, the Belmont Report, and ICH Good Clinical Practice. The study was also approved by the Institutional Review Board (approval no. Si650/2015). All participants were informed about the study and their signed consent forms were obtained. Morning midstream urine samples were collected from 23 healthy subjects (25–50 years). These urine samples with an equal volume (100 ml/each) were then pooled and centrifuged at 2000 × *g* and 4°C for 10 min to eliminate cells and debris. The supernatant was collected and equally divided into 2 main portions: one added with 10 mM sodium azide (NaN_3) and the other without NaN_3 addition. Each portion was then equally aliquoted (30-ml each) and incubated at 25°C for 0, 2, 4, 6, 8 or 24 h (Figure 1A). These aliquots were then investigated as follows.

2.2 | Determination of bacterial contamination in the urine samples

To determine bacterial contamination, urine turbidity and bacterial colony forming unit (CFU) were quantified. Absorbance at λ620 nm was measured using a UV-visible spectrophotometer (Analytik Jena; Jena, Germany) to determine turbidity of the urine samples stored at 25°C for 0, 8 or 24 h with or without NaN_3. The CFU was counted from 10-fold serially diluted 0-h, 8-h and 24-h stored urine samples with or without NaN_3 on Luria-Bertani (LB) (BD Biosciences; San Jose, CA) agar plate. After overnight incubation at 37°C, numbers of bacterial colonies formed on the plate were counted and are reported as CFU/ml urine.

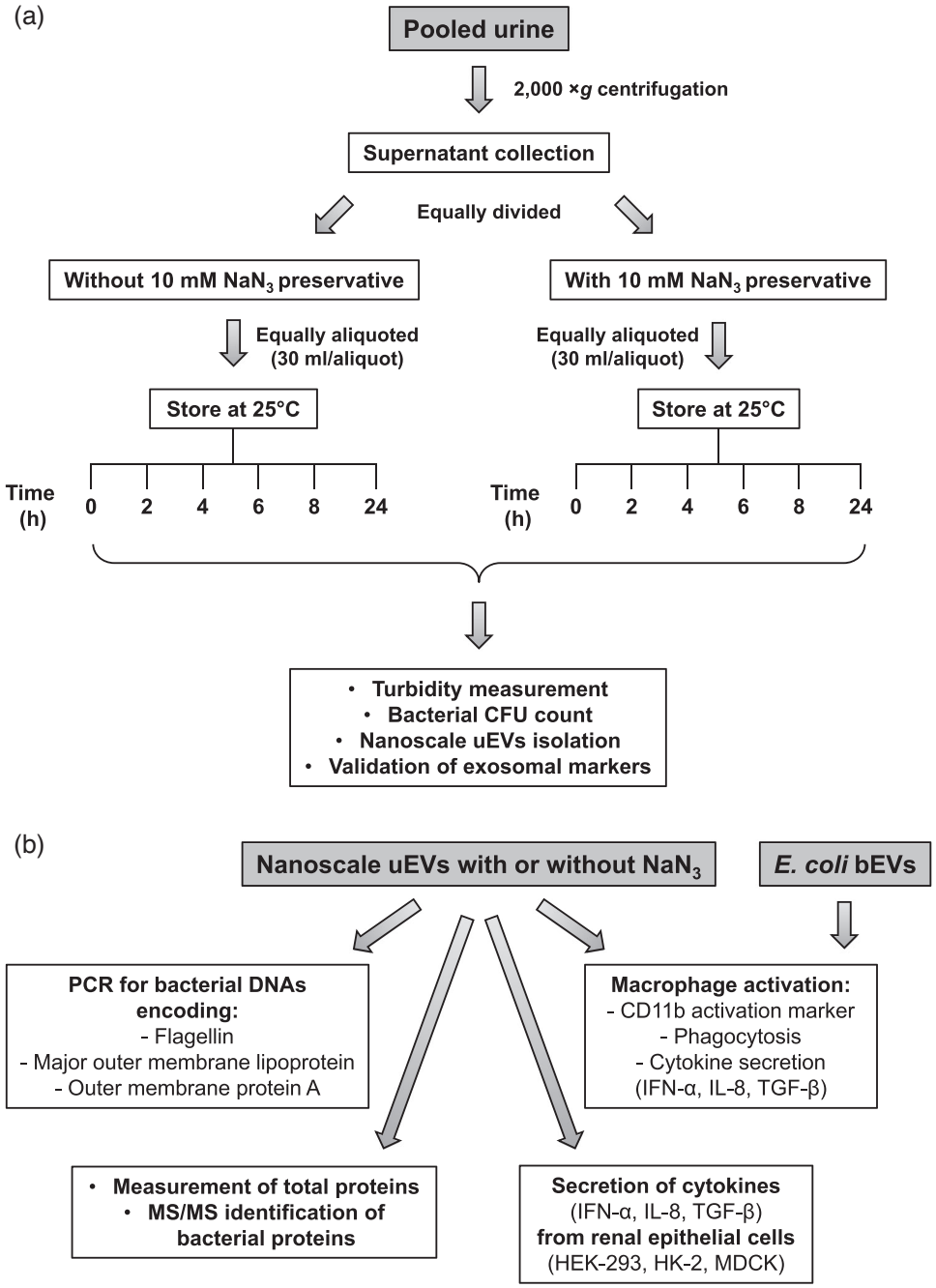

FIGURE 1 Schematic summary of sample preparation and analyses. (A): Urine samples were collected from 23 healthy volunteers, pooled and then subjected to a low-speed centrifugation to remove cells and debris. Thereafter, the pooled samples were divided into two groups (with or without the addition of 10 mM NaN_3), equally aliquoted (30 ml each) and then stored at 25°C. At the indicated time-points, each aliquot was subjected to turbidity measurement, bacterial colony forming unit (CFU) count, nanoscale uEVs isolation, and validation of the nanoscale uEVs enrichment by Western blot analysis of exosomal markers. (B): The nanoscale uEVs samples derived from the urine with or without NaN_3 were then subjected to PCR (to detect bacterial DNAs), total protein measurement, identification of bacterial proteins by tandem mass spectrometry (MS/MS), and several functional assays (to evaluate their effects on macrophage activation marker, phagocytic activity and cytokine secretion, and on the cytokine secretion from various renal cells).

2.3 | Isolation of nanoscale uEVs

At indicated time-points, each aliquot (30-ml each) of the urine with or without NaN_3 prepared as described above (Figure 1A) was centrifuged at 10,000 × *g* for 30 min to remove large EVs (e.g., microvesicles). The obtained supernatant was filtered through a syringe filter (0.22-μm pore size) (Sartorius; Goettingen, Germany) to remove the remaining large EVs and bacteria (if any). Thereafter, the filtrate was ultracentrifuged at 100,000 × *g* and 4°C for 1.5 h to pellet nanoscale uEVs. The enrichment of nanoscale

uEVs, especially exosomes, was validated by Western blot analysis of exosomal markers (see below). Thereafter, the isolated nanoscale uEVs were then subjected to investigations as follows (Figure 1B).

2.4 | Western blotting to validate the enrichment of exosomes after isolation of nanoscale uEVs

The nanoscale uEVs derived from 30-ml aliquot of the basal urine without storage nor NaN_3 were extracted using Laemmli's buffer, whereas the whole basal urine (30-ml) without storage nor NaN_3 was subjected to dialysis against deionized water and concentrated by lyophilization as previously described (Noonin et al., 2021, 2022). Protein concentration in each sample was measured by Bradford's method using Bio-Rad Protein Assay (Bio-Rad Laboratories; Hercules, CA). The nanoscale uEVs and whole urine proteins with an equal amount (40 μg each) were resolved by 12% SDS-PAGE and then transferred to nitrocellulose membranes. The membranes were incubated in PBS containing 5% skim milk for 1 h and then with each of mouse monoclonal antibodies against exosomal markers, including Alix (Jeppesen et al., 2019; Zhao et al., 2021), HSP70 (Singhto et al., 2018), and Rab5 (Singhto & Thongboonkerd, 2018) (all were from Santa Cruz Biotechnology; Santa Cruz, CA), diluted 1:250, 1:1,000 and 1:500, respectively, in PBS containing 1% skim milk at 4°C overnight. After washing with PBS, the membranes were incubated with horseradish peroxidase-conjugated rabbit anti-mouse secondary antibody (Sigma-Aldrich; St. Louis, MO) diluted 1:10,000 in PBS containing 1% skim milk at 25°C for 1 h. The immunoreactive bands were detected using SuperSignal West Pico chemiluminescence substrate (Thermo Scientific; Waltham, MA) and autoradiographic film (X-ray film) (Fujifilm; Tokyo, Japan).

2.5 | Measurement of total proteins in nanoscale uEVs samples

Protein concentrations in individual nanoscale uEVs samples (derived from a 30-ml aliquot per sample) were measured by Bradford's method using Bio-Rad Protein Assay (Bio-Rad Laboratories). The data are then reported as μg of total uEVs proteins per ml of urine.

2.6 | Mass spectrometric (nanoLC-ESI-LTQ-Orbitrap MS/MS) identification of bacterial proteins in nanoscale uEVs samples

Tryptic digestion of nanoscale uEVs proteins derived from 0-h, 8-h and 24-h urine without NaN_3 and 24-h urine with NaN_3 preservation was performed by Filter-Aided Sample Preparation (FASP) protocol (Chaiyarit & Thongboonkerd, 2021; Peerapen & Thongboonkerd, 2020). The digested peptides were then separated by two-column system using nano-flow liquid chromatography EASY-nLC II (Thermo Fisher Scientific; San Jose, CA) as previously described (Peerapen & Thongboonkerd, 2019; Sutthimethakorn & Thongboonkerd, 2020). The peptides were eluted and subjected to analysis by LTQ-Orbitrap-XL (Thermo Scientific) (Thongboonkerd & Chaiyarit, 2022; Yoodee et al., 2021). The MS survey scan was performed in a precursor mass range of 300–2000 m/z with a resolution of 30,000 in the Orbitrap. For MS/MS analysis, the twelve most abundant ions (top-12) in each MS scan with minimum signal threshold at 1×10^5 were selected for fragmentation by collision-induced dissociation (CID) in the linear ion trap. The activation time and dynamic exclusion window were 30 ms and 180 s, respectively.

The MS/MS raw spectra were deconvoluted and then extracted into output searchable *.mgf* files using Proteome Discoverer v.1.4.1.14 software (Thermo Scientific). Mascot software version 2.4.0 (Matrix Science; London, UK) was used to search MS/MS spectra against SwissProt database of bacteria with the following standard Mascot parameters for CID: Enzyme = trypsin, maximal number of missed cleavages = 1, peptide tolerance = ± 2 ppm, MS/MS tolerance = ± 0.1 Da, fixed modification = carbamidomethyl (C), variable modification = oxidation (M), charge state = 2+, and decoy database on false discovery rate (FDR) < 1%.

2.7 | PCR to detect bacterial DNAs in nanoscale uEVs samples

The nanoscale uEVs (from 30-ml aliquot of urine per sample) were suspended in equal volume of PBS and then mixed with primers (listed in Table 1) and reaction mixture containing Taq DNA polymerase (New England BioLabs; Ipswich, MA). The PCR condition was set as follows: 95°C initial denaturation (2 min), 35 cycles of 95°C denaturation (30 s/cycle), 50°C–52°C annealing (30 s), and 68°C extension (30 s), followed by 68°C final extension (5 min). Following agarose gel electrophoresis, the PCR products were stained with RedSafe (iNtRON Biotechnology, Inc.; Seongnam, South Korea) and visualized by using ChemiDoc MP Imaging System (Bio-Rad Laboratories).

TABLE 1 All primers used for PCR in this study

Protein encoded by the target gene	Primers	Sequences (5′ to 3′)	Product size (bp)*	Species specificity
Flagellin	Forward Reverse	GCGTATTAACAGCGCGA TCATTTGCGCCAACCTGGAT	348	*Escherichia coli* *Salmonella enterica* *Serratia marcescens* *Shigella flexneri*
	Forward Reverse	ATGGCACAAGTCATTAATAC CAGGACTTTCACGCCGT	414	*Escherichia coli* *Salmonella enterica* *Serratia marcescens* *Shigella flexneri*
Outer membrane protein A	Forward Reverse	CCATGAAAACCAACTGGGCG TTGGTCTGTACTTCCGGTGC	486-498	*Escherichia coli* *Salmonella enterica* *Shigella flexneri*
	Forward Reverse	TGAATGCGGCTCCGAAAGAT AGTGCTTGGTAGCCACTTCC	588-600	*Salmonella enterica* *Shigella flexneri*
Major outer membrane lipoprotein	Forward Reverse	CAGACGCTGGTTAGCACGAG GCGGTAATCCTGGGTTCTACT	180	*Escherichia coli* *Salmonella enterica* *Shigella flexneri*

*bp = base pair.

For genes encoding flagellin and outer membrane protein A, two pairs of primers (Table 1) were used for their amplification. The band detected after amplifying with any pair was considered as positive result.

2.8 | Isolation of *E. coli* bEVs

A colony of *E. coli* (ATTC 25922) (ATCC; Manassas, VA) grown on LB agar plate was inoculated in LB broth and incubated at 37°C overnight. The inoculum was diluted 1:10 with fresh LB broth and cultured at 37°C for 3 h to reach the late-log phase (absorbance at λ620 nm was approximately 0.9). Then, the suspension was centrifuged at 10,000 ×*g* for 30 min to pellet bacteria. To ensure that the collected supernatant was free of bacterial cells, the supernatant was filtered through 0.22-μm syringe filter (Sartorius). The filtrate (*namely "cell-free cultured medium"*) was subjected to bEVs isolation by centrifugation at 100,000 × *g* and 4°C for 1.5 h. The enrichment of *E. coli* bEVs in the obtained pellet was confirmed by Western blotting as described above but using 20 μg proteins from cell-free cultured medium and from the bEVs pellet, whereas the primary antibody was mouse monoclonal antibody against GroEL (Santa Cruz Biotechnology), one of the bEVs proteins (Hong et al., 2019; Kanlaya et al., 2019). Finally, the obtained *E. coli* bEVs pellet was suspended in RPMI 1640 medium (Gibco; Grand Island, NY) to treat macrophages as follows.

2.9 | Macrophage and renal cell culture and intervention with nanoscale uEVs or *E. coli* bEVs

The impact of the contaminated bEVs on immunomodulatory effects of human nanoscale uEVs was examined in macrophages and renal cells. Macrophages were derived from human monocytic cells as previously described (Singhto & Thongboonkerd, 2018; Sintiprungrat et al., 2010). Briefly, U-937 (ATCC) cells were cultured in RPMI 1640 medium (Gibco) supplemented with 10% (v/v) fetal bovine serum (FBS) (Gibco), 60 μg/ml streptomycin (Sigma-Aldrich; St. Louis, MO), and 60 U/ml penicillin G (Sigma-Aldrich). The cells were seeded into 6-well plate (5×10^5 cells/well) and treated with 100 ng/ml phorbol-12-myristate-13-acetate (PMA) (Fluka; St. Louis, MO) for 48 h. The culture supernatant and non-adhered cells were removed, whereas the adhered cells were washed with PBS and recovered in RPMI supplemented with 10% FBS for 48 h before being treated with nanoscale uEVs or *E. coli* bEVs.

Three renal cell lines, including HEK-293 (human embryonic cells), HK-2 (human proximal tubular cells), and MDCK (canine distal tubular cells) (all were from ATCC) were cultured in Dulbecco's Modified Eagle Medium (DMEM) (Gibco) supplemented with 10% (v/v) FBS, 60 μg/ml streptomycin, and 60 U/ml penicillin G.

All of the cells mentioned above were seeded in 6-well plate (1.5×10^5 cells/well) and incubated in their corresponding culture medium supplemented with 10% FBS as aforementioned for 24 h. At 24 h after plating, the culture medium was removed and the cells were washed with PBS to remove the remaining FBS. Thereafter, the cells were incubated in their corresponding serum-free culture medium added with nanoscale uEVs (derived from 30-ml aliquot of urine stored at 25°C for 0, 8 or 24 h without or with NaN_3) or *E. coli* bEVs (10, 20 or 40 μg/well) at 37°C for 16 h. The effects of nanoscale uEVs with or without NaN_3 preservation and bEVs on macrophages and renal cells were examined as follows (Figure 1B).

2.10 | Flow cytometry to quantify macrophage activation marker

After intervention with nanoscale uEVs or bEVs for 16 h as described above, macrophages were trypsinized and fixed with 4% (w/v) paraformaldehyde at 25°C for 15 min (without permeabilization). Immunofluorescence staining of cell surface CD11b (a macrophage activation marker) and flow cytometric quantification were performed as described previously (Pongsakul et al., 2016; Singhto et al., 2018). Briefly, the cells were incubated with 5% bovine serum albumin (BSA) (Sigma-Aldrich) dissolved in PBS at 25°C for 30 min (to block non-specific binders) and then with mouse monoclonal anti-CD11b antibody (Santa Cruz Biotechnology) or isotype IgG (Santa Cruz Biotechnology) (both were diluted 1:50 in 1% BSA/PBS) at 25°C for 1 h. After washing with PBS, the cells were incubated with Alexa Flour 488-conjugated donkey anti-mouse IgG secondary antibody (Invitrogen/Molecular Probes; Burlington, Canada) (1:500 in 1% BSA/PBS) at 25°C for 1 h and then washed with PBS. The CD11b-positive cells were then analyzed and quantified using a flow cytometer (BD Accuri C6) (BD Biosciences).

2.11 | Phagocytosis assay

After intervention with nanoscale uEVs or bEVs for 16 h as described above, macrophages were subjected to phagocytosis assay as described previously (Singhto et al., 2013, 2018). Briefly, macrophages in each well were incubated at 37°C for 1 h with *Saccharomyces cerevisiae* (2×10^7 cells/well) suspended in RPMI medium supplemented with 10% FBS. Thereafter, the non-phagocytosed yeasts were washed out using PBS, whereas the phagocytic macrophages with yeasts inside were imaged under ECLIPSE-Ti-S inverted phase-contrast light microscope (Nikon). Number of the phagocytic cells and phagocytosed yeasts were counted from 15 random fields/well. % phagocytic cells and % phagocytic index were then calculated using the following formulas.

$$\%\,\text{phagocytic cells} = \left(\text{phagocytic cell number}/\text{total cell number}\right) \times 100 \tag{1}$$

$$\%\,\text{phagocytic index} = \left(\text{phagocytosed yeast number}/\text{total cell number}\right) \times 100 \tag{2}$$

2.12 | ELISA to measure cytokine levels

After intervention with nanoscale uEVs or bEVs for 16 h as described above, ELISA was performed as previously described (Gallemit et al., 2021; Yoodee et al., 2021). Briefly, the conditioned cultured medium from macrophages or renal cells was collected and centrifuged at 500 × *g* for 10 min to remove cells and debris. Subsequently, the supernatant was dialyzed against deionized water followed by lyophilization. Dried proteins from each sample were dissolved in an equal volume of a coating buffer containing 15 mM $NaCO_3$ and 30 mM $NaHCO_3$, pH 9.6. Then, an equal volume of the dissolved proteins was added into each well of 96-well ELISA plate (Nunc; Roskilde, Denmark) and incubated at 4°C overnight to allow the proteins to adhere onto the well surface. After removing non-adhered proteins by washing with 0.05% Tween-20/PBS, 5%BSA/PBS was added and incubated at 25°C for 2 h. Thereafter, each well was incubated with each of these primary antibodies, including mouse monoclonal anti-IFN-α, rabbit anti-IL-8, and mouse monoclonal anti-TGF-β antibodies (all were from Santa Cruz Biotechnology) (5 μg/ml in 0.1% BSA/PBS), at 25°C for 2 h. After washing with PBS, the sample was further incubated with HRP-conjugated rabbit anti-mouse IgG (Sigma-Aldrich) or swine anti-rabbit IgG (Dako; Glostrup, Denmark) secondary antibody at 25°C for 2 h. After washing with PBS, the HRP-substrate solution (3.3 mM ortho-phenylenediamine dihydrochloride (Sigma-Aldrich), 0.012% H_2O_2, 35 mM citric acid monohydrate, and 100 mM Na_2HPO_4, pH 5) was added. The colour was allowed to develop at 25°C in the dark for 15 min before the reaction was stopped by using 2 M H_2SO_4 solution. The absorbance (optical density or OD) of the sample was measured at λ492 nm using an ELISA plate reader (EZRead 400) (Biochrom; Cambridge, UK).

2.13 | Statistical analysis

Three experimental sets were performed for all experiments using independent samples. All quantitative data are reported as mean ± SD. Normality of the dataset was evaluated by using Kolmogorov-Smirnov test. For normally distributed datasets, ANOVA followed by Tukey's (for those with equal variance) or Dunnett's T3 (for those with unequal variance) post-hoc multiple comparisons were performed. Otherwise, the nonparametric Kruskal-Wallis test was performed followed by Dunn's multiple comparisons. Statistically significant differences among experimental groups were considered when p values were less than 0.05.

3 | RESULTS

3.1 | Bacterial overgrowth in the urine and contamination of bacterial proteins and DNAs in human nanoscale uEVs samples

To investigate whether improper storage of the urine (i.e., prolonged storage at room temperature without preservatives) could lead to contamination of bEVs in the isolated nanoscale uEVs, we first determined bacterial overgrowth and the presence of bacterial proteins and DNAs in such improperly stored urine samples. NaN_3 was used as a representative preservative in this study and its concentration used herein was within the range recommended by a previous urinary whole proteome study (Thongboonkerd & Saetun, 2007). The analysis revealed that urine turbidity and bacterial number (CFU/ml) significantly increased when the urine samples were stored at 25°C for 8 h (*namely "8-h urine"*) without NaN_3 and markedly increased when the urine samples were stored at 25°C for 24 h (*namely "24-h urine"*) without NaN_3 (Figure 2A and B). However, those stored with NaN_3 had no significant increases in their turbidity and bacterial number as compared with their baseline samples (*namely "0-h urine"*) (Figure 2A and B). These data indicate the presence of bacterial overgrowth in the 8-h and 24-h urine without NaN_3.

The nanoscale uEVs were then isolated from these urine samples and their enrichment were confirmed by Western blotting using monoclonal antibodies specific for exosomal markers, including Alix, HSP70 and Rab5 (Figure 2C). Measurement of total proteins in each sample revealed that the total protein level significantly increased in the uEVs samples derived from 8-h urine without NaN_3 preservation and dramatically increased in the uEVs samples derived from 24-h urine without NaN_3 preservation, whereas the level in those derived from 24-h urine stored with NaN_3 remained unchanged (Figure 2D). This result implicates that the dramatic increase in total proteins in uEVs derived from 8-h and 24-h urine without NaN_3 was most likely from the contaminated bEVs in these samples.

We also investigated whether appropriate storage of the urine (i.e., at −80°C) immediately after collection and removal of cells and debris could prevent bacterial overgrowth. The data confirmed that urine turbidity and bacterial number remained at their basal levels even after storage at −80°C for 10 days (Supplementary Figure S1A and S1B). Moreover, total protein level in the nanoscale uEVs samples derived from the urine stored at −80°C for 10 days did not change (Supplementary Figure S1C), implicating the absence of bacterial overgrowth in these properly stored urine samples.

Tandem mass spectrometry (nanoLC-ESI-LTQ-Orbitrap MS/MS) was then performed to identify bacterial proteins in the nanoscale uEVs samples derived from 0-h, 8-h and 24-h urine without NaN_3 and 24-h urine with NaN_3 preservation. The data confirmed the presence of 6 and 13 bacterial proteins in the contaminated uEVs samples derived from 8-h and 24-h urine without NaN_3, respectively, whereas none of the bacterial proteins were detected in the uEVs samples derived from 0-h urine without NaN_3 and 24-h urine with NaN_3 (Table 2). Additionally, PCR was performed to confirm the presence of bacterial DNAs in these contaminated samples. As shown in Figure 3, the intense bands of PCR amplicons of the genes encoding flagellin, outer membrane protein A, and major outer membrane lipoprotein (Table 1) were detected in the uEVs samples isolated from 24-h urine without NaN_3. Moreover, a faint band of the gene encoding flagellin was also detected in the uEVs samples isolated from 8-h urine without NaN_3 (Figure 3A), indicating the existence of a small amount of bEVs at this early time-point. These results indicate that the longer the urine was stored at 25°C without preservative, the more bEVs contamination in the uEVs detected. By contrast, there were no PCR bands detected in any of the uEVs samples isolated from 0-h to 24-h urine with NaN_3 (Figure 3).

3.2 | Effects of contaminated nanoscale uEVs and isolated *E. coli* bEVs on macrophage activation marker

After confirming the contamination of bEVs in human nanoscale uEVs samples, we hypothesized that such contamination could lead to an activation of immune cells, thereby interfering with the functional study of the uEVs. Effects the contaminated nanoscale uEVs on macrophage activation were then examined. Flow cytometric analysis revealed the upregulation of

TABLE 2 Summary of bacterial proteins identified in nanoscale uEVs derived from 0-h, 8-h and 24-h urine without NaN_3 and 24-h urine with NaN_3 preservation by nanoLC-ESI-LTQ-Orbitrap MS/MS

SwissProt ID	Protein name	Gene name	Species	MS/MS score	MW (kDa)	No. of distinct peptides/No. of matched peptides	Cov (%)*	pI
uEVs derived from 0-h urine without NaN_3								
No bacterial protein was identified								
uEVs derived from 8-h urine without NaN_3								
P49433	Glyceraldehyde-3-phosphate dehydrogenase 1	*gap1*	*Synechocystis sp*. (strain PCC 6803 / Kazusa)	93	36.408	2/4	7.4	5.86
Q89AK1	Glyceraldehyde-3-phosphate dehydrogenase	*gapA*	*Buchnera aphidicola* subsp. *Baizongia pistaciae* (str. Bp)	93	37.01	1/3	5.1	8.50
Q7V9G2	Chaperone protein dnaK2	*dnaK2*	*Prochlorococcus marinus* (str. SARG / CCMP1375 / SS120)	88	68.36	3/12	4.6	4.78
A5EYG3	Chaperone protein DnaK	*dnaK*	*Dichelobacter nodosus* (str. VCS1703A)	88	69.77	1/10	2.5	4.77
Q4A5Q4	Spermidine/putrescine import ATP-binding protein PotA	*potA*	*Mycoplasma synoviae* (str. 53)	39	53.94	3/8	3.9	8.17
A0KGH7	tRNA pseudouridine synthase D	*truD*	*Aeromonas hydrophila* subsp. *hydrophila* (strain ATCC 7966 / DSM 30187 / BCRC 13018 / CCUG 14551 / JCM 1027 / KCTC 2358 / NCIMB 9240 / NCTC 8049)	31	38.60	1/1	2.6	6.23

(Continues)

TABLE 2 (Continued)

SwissProt ID	Protein name	Gene name	Species	MS/MS score	MW (kDa)	No. of distinct peptides/No. of matched peptides	Cov (%)*	pI
uEVs derived from 24-h urine without NaN_3								
P13713	Flagellin	*fliC*	*Serratia marcescens*	178	36.84	1/6	4.3	4.85
P24017	Outer membrane protein A	*ompA*	*Klebsiella pneumoniae*	52	37.15	8/11	32.3	5.73
Q5PH62	Major outer membrane lipoprotein Lpp 3	*lpp3*	*Salmonella paratyphi* A (str. ATCC 9150 / SARB42)	34	8.52	2/3	30.4	9.18
Q5PH64	Major outer membrane lipoprotein Lpp 1	*lpp1*	*Salmonella paratyphi* A (str. ATCC 9150 / SARB42)	34	8.44	2/3	30.8	9.36
Q8Z6K1	Major outer membrane lipoprotein Lpp 2	*lpp2*	*Salmonella typhi*	34	8.59	2/3	30.4	9.18
P02938	Major outer membrane lipoprotein Lpp	*lpp*	*Serratia marcescens*	34	8.29	2/3	31.2	8.93
C0Q2R3	50S ribosomal protein L11	*rplK*	*Salmonella paratyphi* C (str. RKS4594)	25	14.92	2/4	16.9	9.64
Q1CI1T4	Elongation factor Tu 2	*tuf2*	*Yersinia pestis* bv. Antiqua (str. Antiqua)	24	43.31	6/8	15.7	5.13
Q1CN86	Elongation factor Tu 1	*tuf1*	*Yersinia pestis* bv. Antiqua (str. Nepal516)	24	43.33	6/8	15.7	5.13
Q8ZAN8	Elongation factor Tu-B	*tufB*	*Yersinia pestis*	24	43.31	6/8	15.7	5.13
A6TEX7	Elongation factor Tu	*tufA*	*Klebsiella pneumoniae* subsp. *pneumoniae* (str. ATCC 700721 / MGH 78578)	24	43.39	6/8	15.7	5.29
A6THB4	50S ribosomal protein L9	*rplI*	*Klebsiella pneumoniae* subsp. *pneumoniae* (str. ATCC 700721 / MGH 78578)	22	15.78	2/2	14.8	6.16
Q16D32	Ubiquinone biosynthesis O-methyltransferase	*ubiG*	*Roseobacter denitrificans* (str. ATCC 33942 / OCh 114)	16	27.66	1/1	3.6	5.17
uEVs derived from 24-h urine with NaN_3								
No bacterial protein was identified								

*Cov(%) = (number of the identified amino acid residues/number of amino acid residues in the protein sequence) × 100.

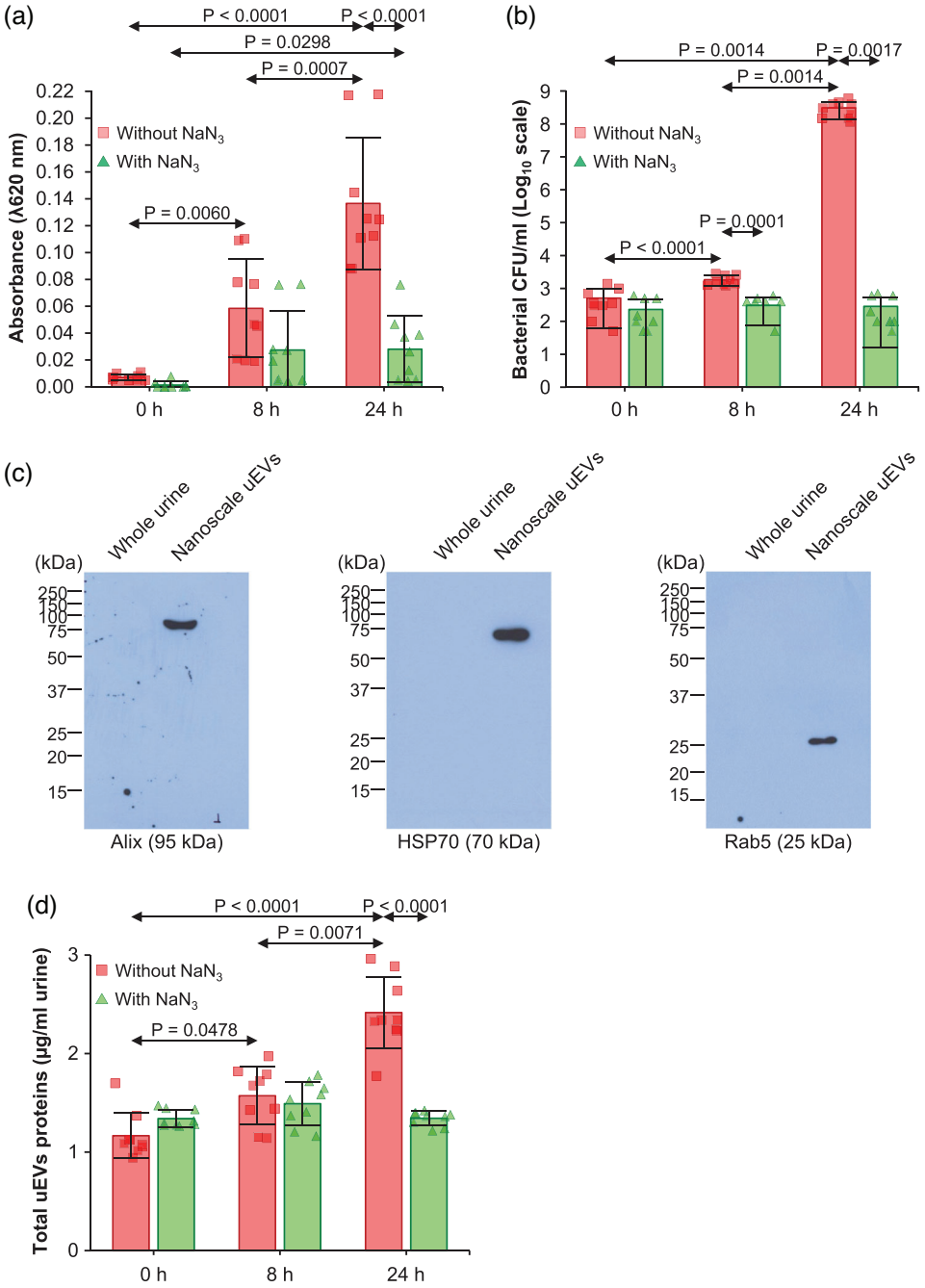

FIGURE 2 Bacterial overgrowth in the urine and contamination of bacterial proteins in human nanoscale uEVs samples. (A) and (B): After removal of cells and debris, the urine samples (30 ml/aliquot) with or without 10 mM NaN_3 were immediately (0 h) subjected to turbidity measurement and bacterial colony forming unit (CFU) count, or stored at 25°C for 8 or 24 h before these measurements. (C): The nanoscale uEVs were then isolated from these urine samples and their enrichment was confirmed by Western blot analysis of exosomal markers, including Alix, HSP70 and Rab5. (D): The amounts of total proteins were measured from nanoscale uEVs samples derived from the urine immediately after collection (0 h) or stored at 25°C for 8 or 24 h with or without NaN_3. All quantitative data were derived from three independent experiments using different biological samples (each with triplicate measurements) and are reported as mean ± SD.

CD11b, a macrophage activation marker, on the cell surface of macrophages treated with nanoscale uEVs derived from 8-h and 24-h urine without NaN_3 in a time-dependent manner (Figure 4A and B). However, the level of CD11b could be preserved at its basal level in macrophages treated with nanoscale uEVs derived from 24-h urine in the presence of NaN_3 (Figure 4A and B). bEVs were then isolated from a reference *E. coli* strain and their enrichment was confirmed by Western blot analysis of GroEL (Figure 4C). Macrophages treated with bEVs also showed upregulation of their surface CD11b expression in a concentration-dependent manner (Figure 4D and E), consistent with the data obtained from the contaminated uEVs.

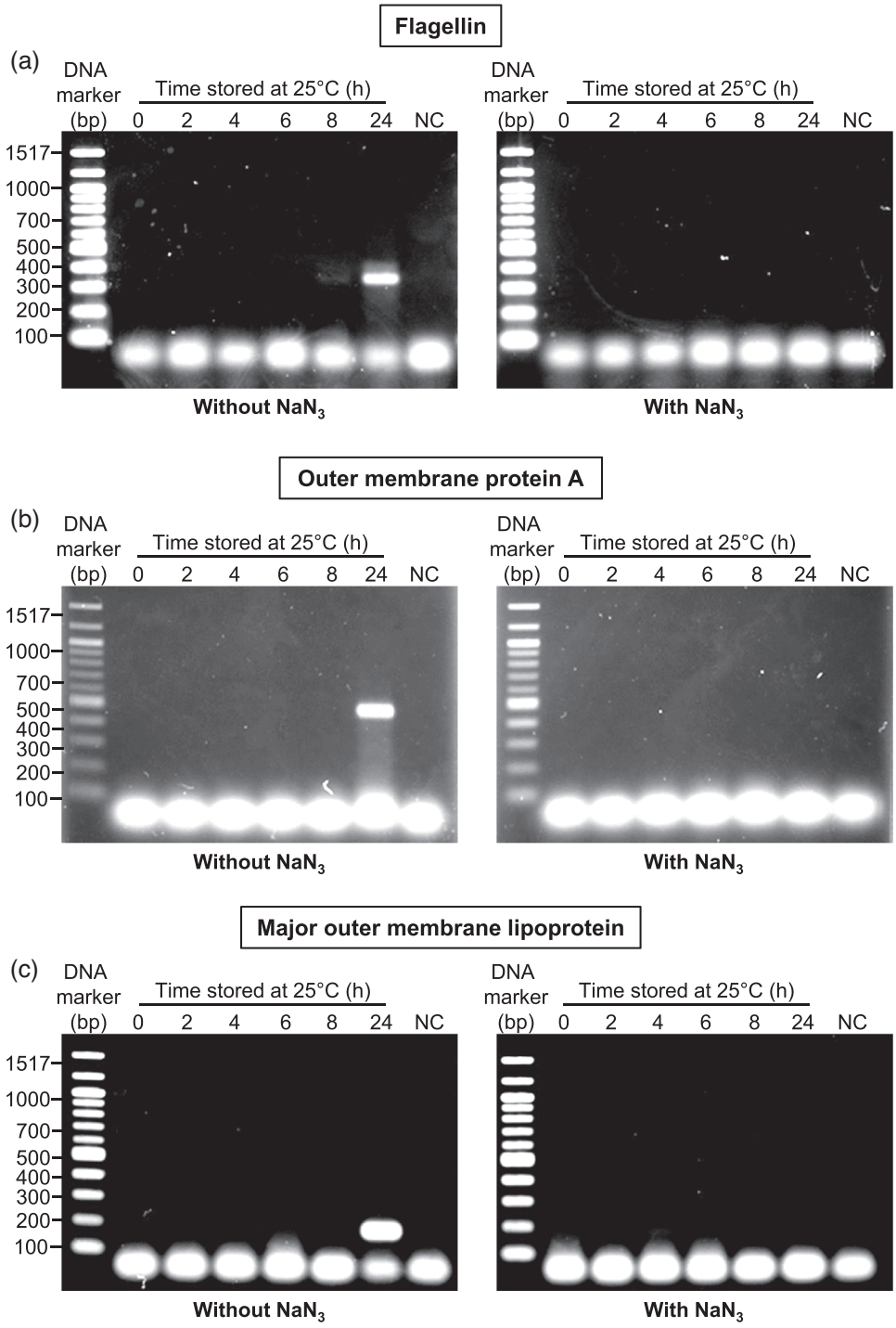

FIGURE 3 Contamination of bacterial DNAs in human nanoscale uEVs samples. After removal of cells and debris, the urine samples (30 ml/aliquot) were stored at 25°C with or without 10 mM NaN_3 for up to 24 h. (A)–(C): At the indicated time-points, nanoscale uEVs were isolated from these samples and subjected to PCR to detect bacterial DNAs encoding flagellin, outer membrane protein A, and major outer membrane lipoprotein, respectively (see additional details in Table 1). bp = base pair; NC = negative control for PCR.

3.3 | Effects of contaminated nanoscale uEVs and isolated *E. coli* bEVs on macrophage phagocytic activity

Effects of the contaminated nanoscale uEVs on macrophage phagocytic activity were then examined. The data demonstrated that both % phagocytic cells (see Formula 1) and % phagocytic index (see Formula 2) were significantly increased by nanoscale uEVs derived from 8-h and 24-h urine without NaN_3 in a time-dependent manner (Figure 5A–C). However, the macrophage

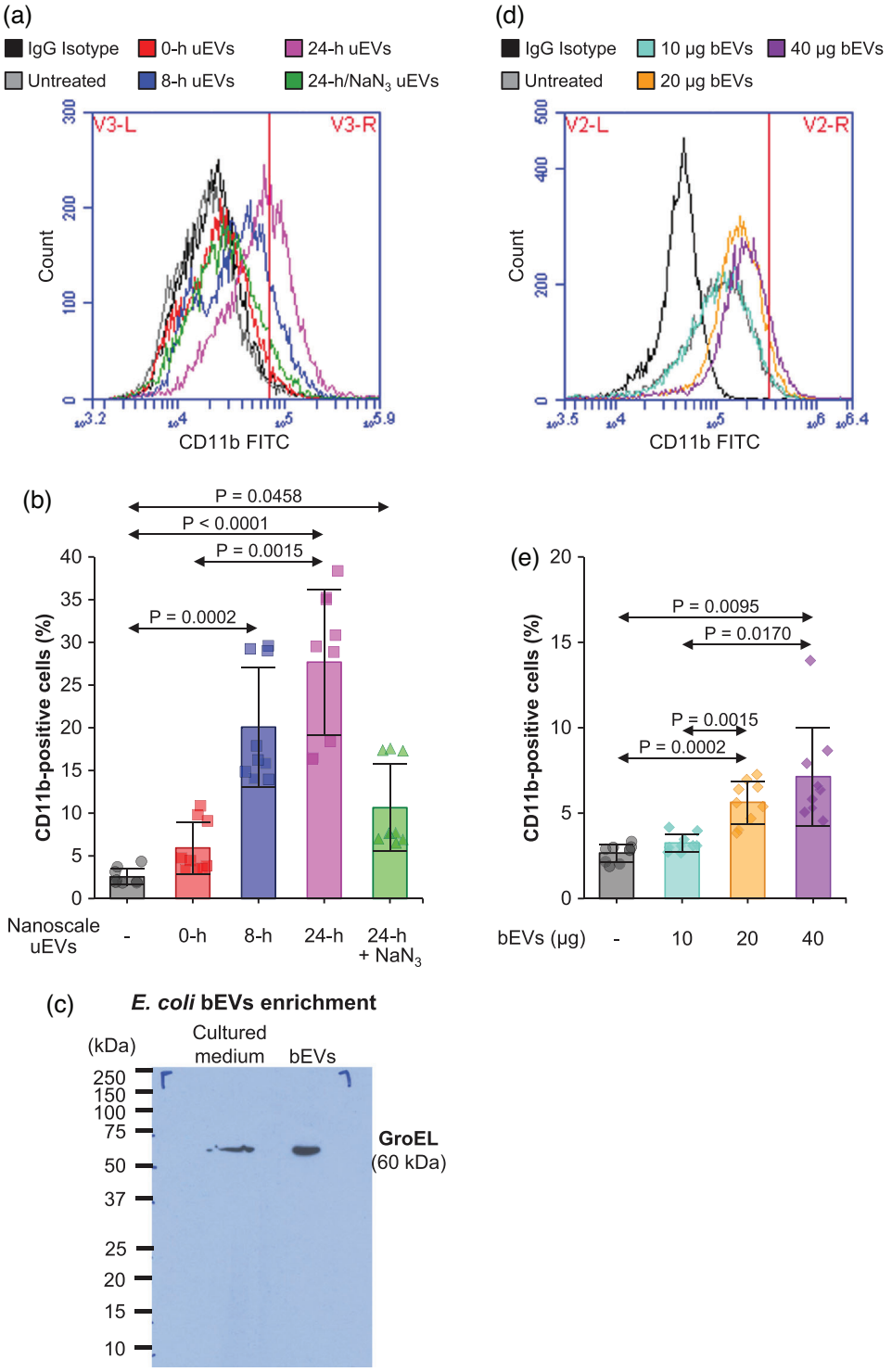

FIGURE 4 Effects of contaminated nanoscale uEVs and isolated *E. coli* bEVs on macrophage activation marker. (A)–(B): After removal of cells and debris, the urine samples (30 ml/aliquot) were stored at 25°C with or without 10 mM NaN_3. At the indicated time-points, nanoscale uEVs were isolated from these samples and incubated with U937-derived macrophages for 16 h followed by flow cytometric analysis of the surface expression of CD11b, a macrophage activation marker. (C): Bacterial extracellular vesicles (bEVs) secreted from *E. coli* were purified and their enrichment was confirmed by Western blot analysis of an outer membrane vesicular protein, GroEL. (D)–(E): *E. coli* bEVs at various concentrations (10-40 μg/well) were incubated with U937-derived macrophages for 16 h followed by flow cytometric analysis of the surface expression of CD11b. Macrophages unexposed to nanoscale uEVs nor *E. coli* bEVs served as the untreated controls (grey lines, bars and dots). All quantitative data were derived from three independent experiments using different biological samples (each with triplicate measurements) and are reported as mean ± SD.

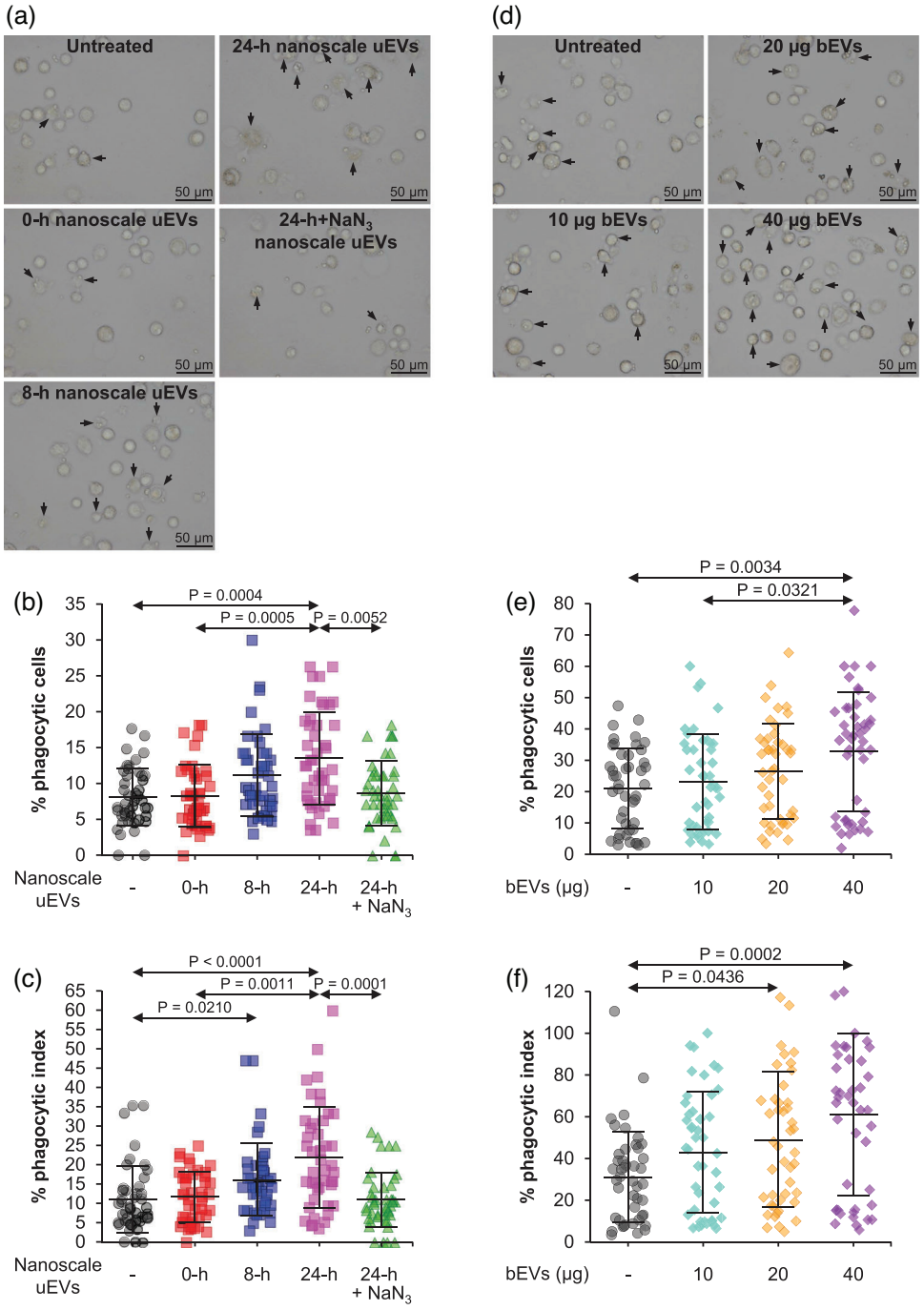

FIGURE 5 Effects of contaminated nanoscale uEVs and isolated *E. coli* bEVs on macrophage phagocytic activity. (A)–(C): After removal of cells and debris, the urine samples (30 ml/aliquot) were stored at 25°C with or without 10 mM NaN_3. At the indicated time-points, nanoscale uEVs were isolated from these samples and incubated with U937-derived macrophages for 16 h followed by phagocytosis assay to evaluate the phagocytic activity. % phagocytic cells and % phagocytic index (see Formula 1 and Formula 2 in Materials and Methods) were calculated from 15 random fields/well from each biological sample. (D)–(F): *E. coli* bEVs at various concentrations (10–40 μg/well) were incubated with U937-derived macrophages for 16 h followed by phagocytosis assay to evaluate the phagocytic activity as for the uEVs experiment. Macrophages unexposed to nanoscale uEVs nor *E. coli* bEVs served as the untreated controls (grey dots). Arrow heads in (A) and (D) indicate the phagocytic cells. All quantitative data were derived from three independent experiments using different biological samples and are reported as mean ± SD.

phagocytic activity could be preserved at the basal level in the cells treated with nanoscale uEVs derived from 24-h urine in the presence of NaN_3 (Figure 5A–C). Similar to the expression of CD11b, both % phagocytic cells and % phagocytic index were significantly increased by bEVs in a concentration-dependent manner (Figure 5D–F).

3.4 | Effects of contaminated nanoscale uEVs and isolated *E. coli* bEVs on cytokine secretion from macrophages

In addition, secretion of cytokines from macrophages was evaluated by ELISA. The results demonstrated that nanoscale uEVs derived from 8-h urine without NaN_3 significantly induced secretion of IFN-α, IL-8 and TGF-β, whereas those derived from 24-h urine without NaN_3 induced only TGF-β (Figure 6A–C). Interestingly, levels of IL-8 and TGF-β, but not that of IFN-α, could be partially preserved by nanoscale uEVs derived from 24-h urine with NaN_3 preservation. bEVs also exerted the concentration-dependent stimulatory effects on secretion of IFN-α and TGF-β by macrophages (Figure 6D and F). Unlike the others, the highest level of IL-8 secretion was observed when macrophages were treated with 20 μg/well bEVs (Figure 6E) (see explanation for these phenomena in the Discussion).

3.5 | Effect of contaminated nanoscale uEVs on cytokine secretion from various renal cells

Furthermore, the effects of the contaminated nanoscale uEVs on secretion of cytokines from renal cells were determined. The nanoscale uEVs derived from 8-h and 24-h urine without NaN_3 time-dependently induced secretion of IFN-α from all renal cells tested, including HEK-293, HK-2 and MDCK cells), whereas NaN_3 could completely or partially preserve the level of IFN-α secretion from these renal cells (Figure 7). For IL-8, nanoscale uEVs derived from 8-h and 24-h urine without NaN_3 significantly induced its secretion from MDCK cells, but only those derived from 24-h urine without NaN_3 significantly induced its secretion from HEK-293 and HK-2, whereas NaN_3 could completely preserve the level of IL-8 secretion from these renal cells. For TGF-β, only nanoscale uEVs derived from 8-h urine without NaN_3 significantly induced its secretion from all these renal cells, whereas NaN_3 partially preserved the level of TGF-β from HEK-293 and HK-2 cells (Figure 7).

4 | DISCUSSION

Urinary tract is known to host various species of bacteria, collectively called "urinary microbiota", which can be found in the normal urine (Aragon et al., 2018; Neugent et al., 2020). Midstream urine collected from healthy individuals contains bacteria $< 10^3$ CFU/ml, whereas that obtained from patients with urinary tract infection (UTI) has bacteria $\geq 10^3$ CFU/ml (Coulthard, 2019; Kranz et al., 2018). In consistent, our present study found that the 0-h urine with or without NaN_3 contained $< 10^3$ CFU/ml bacteria. An existence of urinary microbiota indicates a high possibility of overgrowth of these microbes in the urine samples stored under inappropriate conditions (Thongboonkerd & Saetun, 2007). As expected, prolonged storage at room temperature (25°C) without NaN_3 preservation caused bacterial overgrowth in the sample. By contrast, addition of NaN_3 and immediate storage of the urine samples at −80°C after collection and cell/debris removal successfully prevented bacterial overgrowth in the samples.

bEVs were likely to be secreted from the overgrowth bacteria in the improperly stored urine samples (Bitto et al., 2017; Tulkens et al., 2020). These bEVs have sizes overlapping with those of human nanoscale uEVs and thus are most likely to be co-purified using ultracentrifugation technique (Jeppesen et al., 2019; Tulkens et al., 2020). The presence of bEVs proteins in nanoscale uEVs samples can easily interfere with determination of uEVs protein concentration. Unfortunately, there was no previous report showing this evidence. Our present study therefore provides such direct evidence demonstrating the influence of the contaminated bEVs on uEVs protein measurement (approximately 2-fold increase of the total proteins measured in the contaminated samples). MS/MS analysis of the nanoscale uEVs isolated from 8-h and 24-h urine without preservative confirmed the presence of a number of bacterial proteins in these contaminated samples. Among the identified bacterial proteins, flagellin, outer membrane protein, and major outer membrane lipoprotein are the well-known and common bEVs proteins reported in other studies (Bhar et al., 2021; Hu et al., 2020; Liu et al., 2017; Zwarycz et al., 2020). Additionally, most of bacterial proteins identified in the contaminated uEVs sample belong to bacterial species previously reported as the microbiota in urinary and/or gastrointestinal tracts (Kranz et al., 2018; Liu et al., 2020; Neugent et al., 2020).

In addition to proteins, bEVs also contain other cellular components (DNAs, RNAs, peptidoglycan, etc.) (Bitto et al., 2021; Dagnelie et al., 2020; Hu et al., 2021). PCR in this present study confirmed the presence of bacterial DNAs in the nanoscale uEVs samples derived from the 8-h and 24-h urine without preservation. The existence of bacterial nucleic acids can definitely lead to inaccurate determination of DNA and RNA contents in the uEVs samples. Such inaccuracy can seriously affect interpretation of the data obtained from biomarker discovery and therapeutic studies of the uEVs (Cao et al., 2022; Li et al., 2022; Ugarte et al., 2021; Wang et al., 2022).

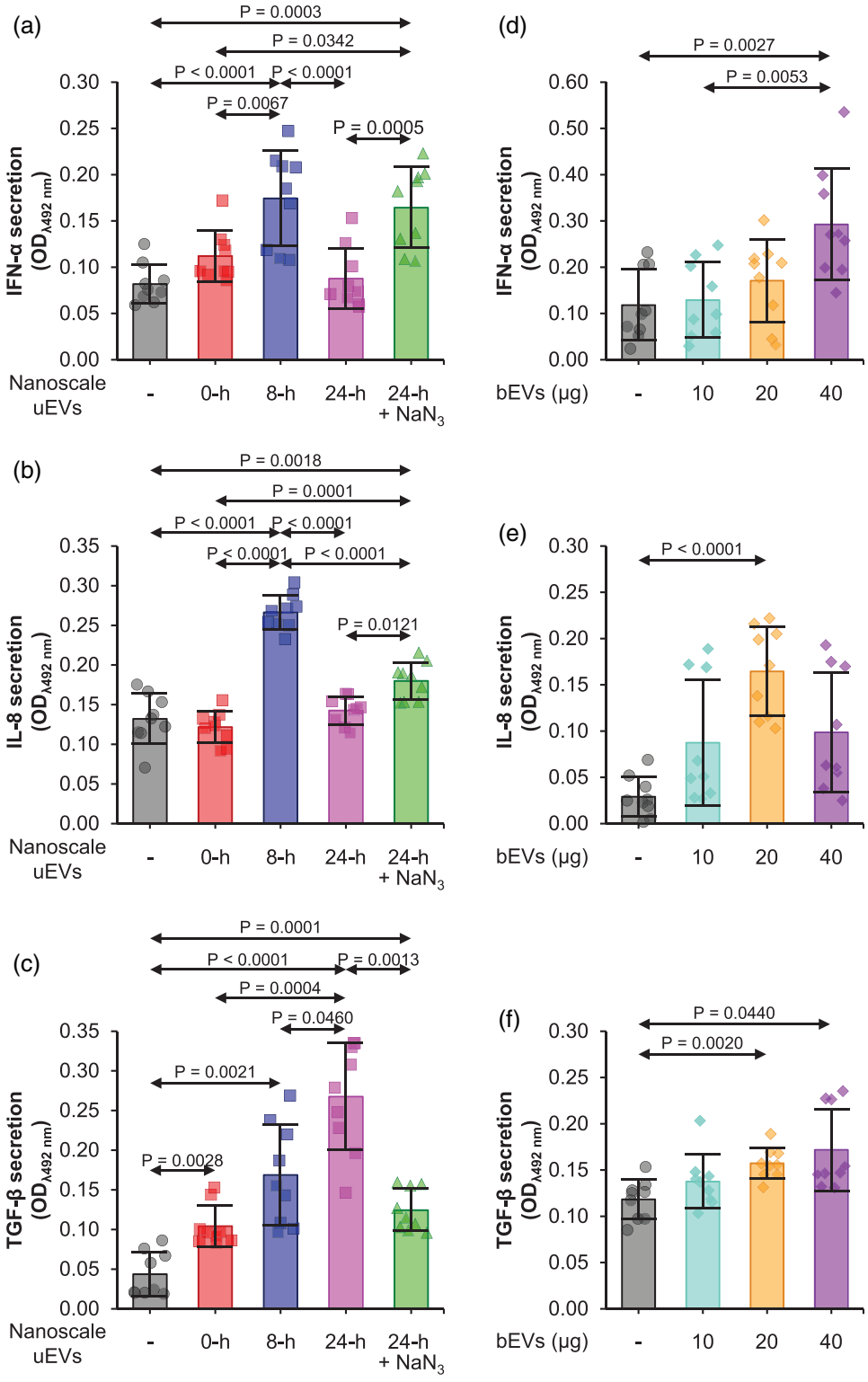

FIGURE 6 Effects of contaminated nanoscale uEVs and isolated *E. coli* bEVs on cytokine secretion from macrophages. (A)–(C): After removal of cells and debris, the urine samples (30 ml/aliquot) were stored at 25°C with or without 10 mM NaN_3. At the indicated time-points, nanoscale uEVs were isolated from these samples and incubated with U937-derived macrophages for 16 h. Thereafter, ELISA was performed to measure levels IFN-α, IL-8 and TGF-β secreted from these macrophages. (D)–(F): *E. coli* bEVs at various concentrations (10–40 μg/well) were incubated with U937-derived macrophages for 16 h. ELISA was then performed to measure levels of IFN-α, IL-8 and TGF-β secreted from these macrophages. Macrophages unexposed to nanoscale uEVs nor *E. coli* bEVs served as the untreated controls (grey bars and dots). All quantitative data were derived from three independent experiments using different biological samples (each with triplicate measurements) and are reported as mean ± SD.

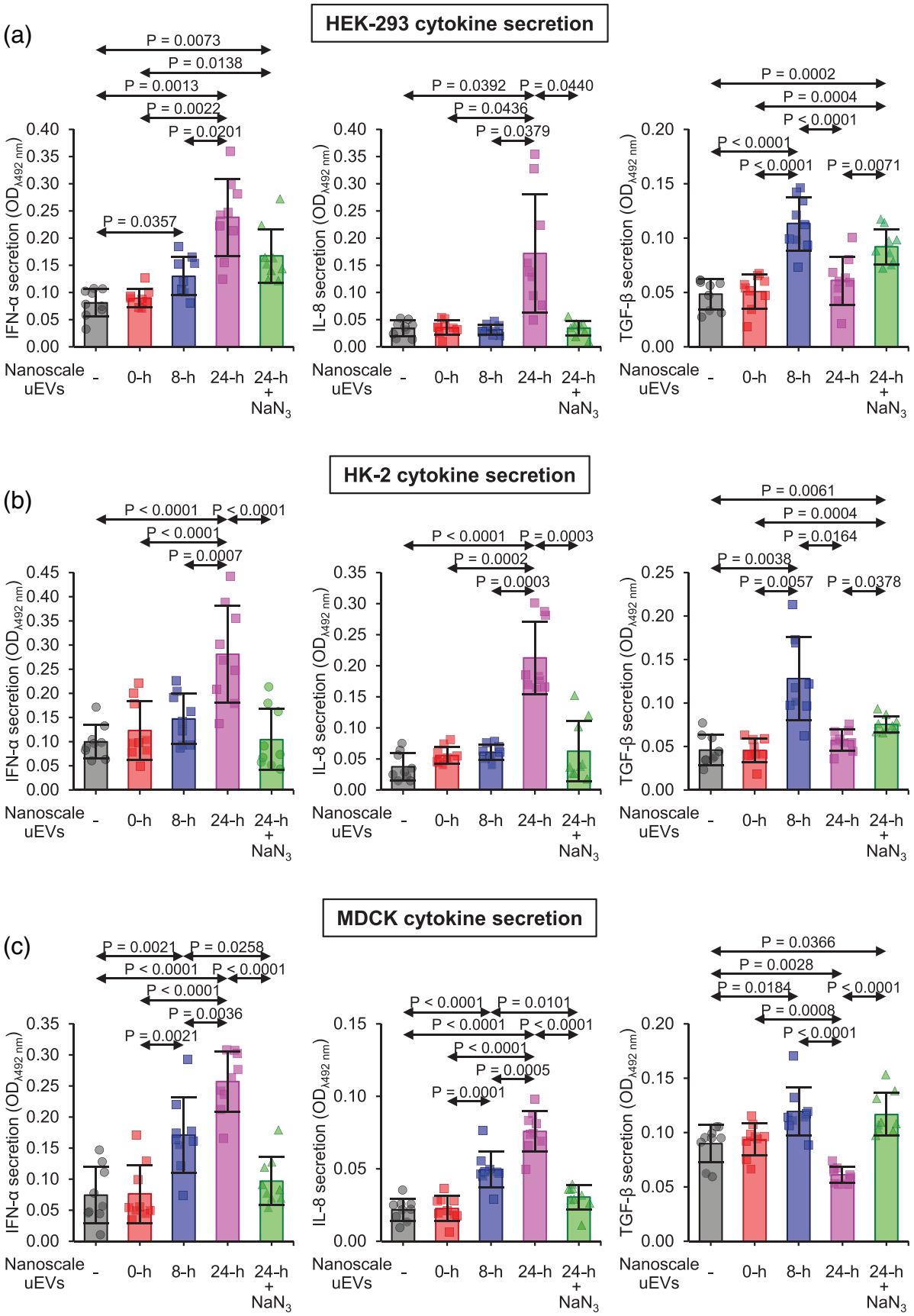

FIGURE 7 Effect of contaminated nanoscale uEVs on cytokine secretion from various renal cells. (A)–(C): After removal of cells and debris, the urine samples (30 ml/aliquot) were stored at 25°C with or without 10 mM NaN_3. At the indicated time-points, nanoscale uEVs were isolated from these samples and

(Continues)

FIGURE 7 (Continued)
incubated with renal cells, including HEK-293, HK-2 and MDCK, for 16 h. ELISA was then performed to measure levels IFN-α, IL-8 and TGF-β secreted from these cells. Renal cells unexposed to nanoscale uEVs served as the untreated controls (grey bars and dots). All quantitative data were derived from three independent experiments using different biological samples (each with triplicate measurements) and are reported as mean ± SD.

The biomolecules carried by both nanoscale uEVs and bEVs can be delivered to host cells and elicit immunomodulating activities for immune and non-immune cells (Canas et al., 2018; Chatterjee & Chaudhuri, 2013; Dagnelie et al., 2020; Gilmore et al., 2021). Because macrophage is an innate immune cell that can be activated by a broad range of microorganisms, it was used as a representative immune cell to demonstrate the immunomodulatory activities of bEVs contaminated in the nanoscale uEVs. Furthermore, the nanoscale uEVs were isolated from the urine. Various renal cells, which have direct contact with the urine, were therefore examined. Our data showed that the bEVs-contaminated nanoscale uEVs and the purified *E. coli* bEVs obviously modulated immune responses in human macrophages and various renal cells. By contrast, nanoscale uEVs isolated from the clean urine sample (0-h) had no or only trivial effects on the immune responses in macrophages and renal cells. This indicates that the changes in immune responses induced by nanoscale uEVs derived from 8-h and 24-h urine without NaN_3 preservation were mainly the results from bEVs contaminated in these samples. It should be noted that there were some degrees of differences in responses to bEVs-contaminated nanoscale uEVs versus *E. coli* bEVs observed in this study. Such differences were possibly due to the differential levels of bEVs present in these samples. Moreover, bEVs produced by different bacterial species or strains carry different components inside their cargos (Bitto et al., 2017, 2021; Zwarycz et al., 2020). While the purified bEVs were solely from *E. coli*, bEVs in the contaminated uEVs samples were from multiple/mixed species. Consequently, responses of the host cells to bEVs from different bacterial species and strains varied (Bitto et al., 2021; Cecil et al., 2017). This could explain some differences observed in cytokine secretion from macrophages induced by bEVs-contaminated nanoscale uEVs versus purified *E. coli* bEVs.

The bEVs-contaminated nanoscale uEVs elicited time-dependent stimulatory effects on macrophage activation as determined by CD11b activation marker and phagocytosis, consistent with the concentration-dependent effects induced by the purified *E. coli* bEVs. However, their effects on macrophage cytokine secretion were somewhat different. The induction of macrophage TGF-β secretion by the contaminated uEVs samples was time-dependent. However, their effects on macrophage IFN-α and IL-8 secretion were maximal with the samples derived from 8-h urine without preservative, whereas the effects from 24-h urine-derived uEVs without preservative decreased to be comparable with those of the 0-h samples. Similar phenomenon was also observed for the purified *E. coli* bEVs. While the stimulatory effects of *E. coli* bEVs on macrophage IFN-α and TGF-β secretion were concentration-dependent as expected, their induction effect on IL-8 secretion was maximal with the amount of 20 μg/well, not 40 μg/well. These results might be explained by the endotoxin tolerance phenomenon, in which the host cells reduce pro-inflammatory response but, on the contrary, increase anti-inflammatory response after repeated exposure to the endotoxin (e.g., lipopolysaccharide or LPS) (Liu et al., 2019; Vergadi et al., 2018). Markers for the pro-inflammatory response include secretion of the pro-inflammatory cytokines such as IFN-α/β, IFN-γ, IL-1β, IL-8, IL-6 and TNF-α (Chen et al., 2018; Lai et al., 2021), while those for the anti-inflammatory response include secretion of the anti-inflammatory cytokines such as IL-4, IL-10 and TGF-β (Castillo et al., 2022; Chen et al., 2018).

The endotoxin tolerance is also exhibited in chicken macrophages exposed to LPS following *L. reuteri* bEVs treatment (Hu et al., 2021). In such macrophages, the up-regulated levels of IL-1β, IL-6 and TNF-α are lower than in those exposed to only LPS. By contrast, expression levels of IL-10 and TGF-β in chicken macrophages exposed to both LPS and *L. reuteri* bEVs are higher than those in macrophages exposed to only LPS (Hu et al., 2021). Besides, concentration of *P. gingivalis* bEVs seems to be a factor causing endotoxin tolerance in monocytes and macrophages treated with *P. gingivalis* bEVs followed by *P. gingivalis* infection (Cecil et al., 2017). An increase in concentration of *P. gingivalis* bEVs results in reduction of IL-1β, IL-8, and TNF-α secretion, but stimulation of IL-10 secretion (Cecil et al., 2017). These findings are consistent with the results observed in our present study.

Exposing immune cells to the anti-inflammatory cytokines like IL-10 and TGF-β contributes to less pro-inflammatory responses of immune cells to the endotoxin (Schroder et al., 2003; Waller et al., 2016). In addition, blocking the functions of IL-10 and TGF-β promotes pro-inflammatory cytokine expression in human colonic mucosa in response to endotoxin exposure (Jarry et al., 2008). In this present study, the highest increase of TGF-β secretion was detected when macrophages were treated with the uEVs samples derived from 24-h urine without NaN_3. Such (maximal) increased level of TGF-β was probably a reason for the blunt effects of the uEVs samples derived from 24-h urine without NaN_3 on macrophage IFN-α and IL-8 secretion. Similar findings were also observed for the effects from the *E. coli* bEVs on macrophage IL-8 secretion. Nevertheless, the TGF-β level induced by 40 μg/well *E. coli* bEVs might not be high enough to elicit their blunt effects on IFN-α secretion from macrophages, thereby the concentration-dependent induction effects were still observed.

It should be noted that NaN_3 could partially preserve the secretory levels of IL-8 and TGF-β from macrophages to their basal levels. However, this was not the case for IFN-α as its secretory level from macrophages treated with the uEVs derived from 24-h urine with NaN_3 was comparable to that induced by the uEVs derived from 8-h urine without NaN_3 preservation. This might be,

at least in part, due to the incomplete inhibition of NaN_3 on the overgrowth of urinary microbiota at 24-h time-point, thereby expressing similar effects as for the 8-h uEVs samples, which contained a milder degree of bEVs contamination.

On the other hand, endotoxin tolerance was not observed in renal cells treated with nanoscale uEVs and *E. coli* bEVs in our present study. Time-dependent induction of the secretion of pro-inflammatory cytokines (IFN-α and IL-8) from all three renal cells was observed after exposure to the uEVs derived from 8-h and 24-h urine without NaN_3 preservation. In concordance, the increased secretion of IL-8 has been reported in intestinal epithelial cells exposed to *C. jejuni* bEVs in a concentration-dependent manner (Elmi et al., 2016). Moreover, bEVs-induced upregulation of IL-6 and IL-8 has been shown in epithelial cells exposed to bEVs isolated from *E. coli* (Canas et al., 2018), *F. nucleatum* (Engevik et al., 2021), *S. aureus* (Bitto et al., 2021), and *V. cholerae* (Chatterjee & Chaudhuri, 2013). These findings are consistent with the data obtained in our present study. For TGF-β, there is no previous evidence reporting the induction effects of uEVs or bEVs on TGF-β secretion from epithelial cells. However, co-treatment of LPS and inactivated *L. plantarum* 22A-3 bacterium has been shown to activate TGF-β secretion from intestinal epithelial cells (Lamubol et al., 2021). In our present study, the nanoscale uEVs with low bEVs contamination (8-h) provided the maximal induction effects on TGF-β secretion from renal cells. However, the uEVs samples derived from 24-h urine without NaN_3 did not seem to induce TGF-β secretion from these renal cells. The lack of stimulatory effects of 24-h nanoscale uEVs on TGF-β secretion from all the renal cells being tested was somewhat unexpected and needs further elucidations.

Herein, we have provided obvious examples that the contaminated bEVs can really affect expression and functional investigations of urinary exosomes or nanoscale uEVs, leading to data misinterpretation. Moreover, these data provide an important point that a tiny amount of the contaminated bEVs can dramatically alter cellular responses. However, it should be noted that the phenomena observed on macrophages and various renal cells, as the effectors, do not necessarily reflect responses of other cells to the contaminated uEVs. Different cell types may have differential responses, which need further elucidations. Last but not least, it should be noted that although HEK-293 cell line was originated from the kidney, this cell line also expresses some neuronal specific proteins (Shaw et al., 2002). Therefore, cautions are to be made for the precise interpretation of datasets.

5 | CONCLUSIONS

This study clearly shows that inappropriate storage of the urine samples results in bacterial overgrowth. As a result, there is the contamination from bEVs derived from various bacterial species in the nanoscale uEVs samples isolated from the improperly stored urine. Such contamination obviously affects purity and quality of the uEVs. Moreover, bacterial proteins, nucleic acids, and other components carried by the contaminated bEVs can easily interfere with the downstream expression and functional investigations of the isolated uEVs. In addition to the inaccurate estimation of the uEVs proteins, we have demonstrated that the bEVs-contaminated uEVs samples derived from the urine stored at room temperature for 8-h and 24-h without any preservative, but not their basal samples at 0-h storage, can abnormally activate the immune responses in macrophages and renal cells. Our data also demonstrate that using 10 mM NaN_3 as a preservative can partially prevent the interfering effects from such bEVs contamination. Therefore, we recommend to add a preservative (e.g., 10 mM NaN_3) into the urine samples when the samples are likely to be stored at room temperature for a certain period. And even though the preservative is added, the samples should not be stored at room temperature for longer than 8-h. Otherwise, the urine should be stored at 4°C or lower (such as at −80°C) soon after the cells and debris were removed following the collection.

AUTHOR CONTRIBUTIONS

Chadanat Noonin: Conceptualization; Data curation; Formal analysis; Investigation; Methodology; Validation; Writing – original draft; Writing – review & editing. Paleerath Peerapen: Conceptualization; Data curation; Formal analysis; Investigation; Methodology; Validation; Writing – review & editing. Visith Thongboonkerd: Conceptualization; Formal analysis; Funding acquisition; Methodology; Project administration; Resources; Software; Supervision; Validation; Writing – original draft; Writing – review & editing.

ACKNOWLEDGEMENTS

We thank Dr. Sakdithep Chaiyarit, Dr. Sirinthorn Sunthornthummas, Ms. Kanyarat Suksakit and Ms. Yanisa Techapaitoonsuk for their technical assistance. This study was supported by Mahidol University research grant.

CONFLICT OF INTEREST

The authors declare no conflict of interest.

ORCID

Visith Thongboonkerd https://orcid.org/0000-0001-7865-0765

REFERENCES

Aragon, I. M., Herrera-Imbroda, B., Queipo-Ortuno, M. I., Castillo, E., Del Moral, J. S., Gomez-Millan, J., Yucel, G., & Lara, M. F. (2018). The urinary tract microbiome in health and disease. *European Urology Focus*, *4*, 128–38.

Bhar, S., Edelmann, M. J., & Jones, M. K. (2021). Characterization and proteomic analysis of outer membrane vesicles from a commensal microbe, *Enterobacter cloacae*. *Journal of Proteomics*, *231*, 103994.

Bitto, N. J., Chapman, R., Pidot, S., Costin, A., Lo, C., Choi, J., D'Cruze, T., Reynolds, E. C., Dashper, S. G., Turnbull, L., Whitchurch, C. B., Stinear, T. P., Stacey, K. J., & Ferrero, R. L. (2017). Bacterial membrane vesicles transport their DNA cargo into host cells. *Scientific Reports*, *7*, 7072.

Bitto, N. J., Cheng, L., Johnston, E. L., Pathirana, R., Phan, T. K., Poon, I. K. H., O'Brien-Simpson, N. M., Hill, A. F., Stinear, T. P., & Kaparakis-Liaskos, M. (2021). Staphylococcus aureus membrane vesicles contain immunostimulatory DNA, RNA and peptidoglycan that activate innate immune receptors and induce autophagy. *Journal of Extracellular Vesicles*, *10*, e12080.

Canas, M. A., Fabrega, M. J., Gimenez, R., Badia, J., & Baldoma, L. (2018). Outer membrane vesicles from probiotic and commensal *Escherichia coli* activate NOD1-mediated immune responses in intestinal epithelial cells. *Frontiers in Microbiology*, *9*, 498.

Cao, Y., Shi, Y., Wang, Y., Yang, Y., Guo, W., Zhang, C., Pei, W., & Fuet, C. (2022). Exosomal hsa_circ_0008925 from urine is related to chronic renal fibrosis. *Disease Markers*, *2022*, 1899282.

Castillo, C., Saez-Orellana, F., Godoy, P. A., & Fuentealba, J. (2022). Microglial activation modulated by P2×4R in ischemia and repercussions in Alzheimer's disease. *Frontiers in Physiology*, *13*, 814999.

Cecil, J. D., O'Brien-Simpson, N. M., Lenzo, J. C., Holden, J. A., Singleton, W., Perez-Gonzalez, A., Mansell, A., & Reynolds, E. C. (2017). Outer membrane vesicles prime and activate macrophage inflammasomes and cytokine secretion in vitro and in vivo. *Frontiers in Immunology*, *8*, 1017.

Chaiyarit, S., & Thongboonkerd, V. (2021). Oxidative modifications switch modulatory activities of urinary proteins from inhibiting to promoting calcium oxalate crystallization, growth, & aggregation. *Molecular & Cellular Proteomics*, *20*, 100151.

Chatterjee, D., & Chaudhuri, K. (2013). Vibrio cholerae O395 outer membrane vesicles modulate intestinal epithelial cells in a NOD1 protein-dependent manner and induce dendritic cell-mediated Th2/Th17 cell responses. *Journal of Biological Chemistry*, *288*, 4299–309.

Chen, L., Deng, H., Cui, H., Fang, J., Zuo, Z., Deng, J., Li, Y., Wang, X., & Zhao, L. (2018). Inflammatory responses and inflammation-associated diseases in organs. *Oncotarget*, *9*, 7204–18.

Chirackal, R. S., Jayachandran, M., Wang, X., Edeh, S., Haskic, Z., Perinpam, M., Halling, T. M., Mehta, R., Rivera, M. E., & Lieske, J. C. (2019). Urinary extracellular vesicle-associated MCP-1 and NGAL derived from specific nephron segments differ between calcium oxalate stone formers and controls. *American Journal of Physiology. Renal Physiology*, *317*, F1475–F82.

Colao, I. L., Corteling, R., Bracewell, D., & Wall, I. (2018). Manufacturing exosomes: A promising therapeutic platform. *Trends in Molecular Medicine*, *24*, 242–56.

Coulthard, M. G. (2019). Defining urinary tract infection by bacterial colony counts: a case for 100,000 colonies/ml as the best threshold. *Pediatric Nephrology*, *34*, 1639–49.

Dagnelie, M. A., Corvec, S., Khammari, A., & Dreno, B. (2020). Bacterial extracellular vesicles: A new way to decipher host-microbiota communications in inflammatory dermatoses. *Experimental Dermatology*, *29*, 22–8.

Elmi, A., Nasher, F., Jagatia, H., Gundogdu, O., Bajaj-Elliott, M., Wren, B., & Dorrell, N. (2016). Campylobacter jejuni outer membrane vesicle-associated proteolytic activity promotes bacterial invasion by mediating cleavage of intestinal epithelial cell E-cadherin and occludin. *Cellular Microbiology*, *18*, 561–72.

Engevik, M. A., Danhof, H. A., Ruan, W., Engevik, A. C., Chang-Graham, A. L., Engevik, K. A., Shi, Z., Zhao, Y., Brand, C. K., Krystofiak, E. S., Venable, S., Liu, X., Hirschi, K. D., Hyser, J. M., Spinler, J. K., Britton, R. A., & Versalovic, R. A. (2021). Fusobacterium nucleatum secretes outer membrane vesicles and promotes intestinal inflammation. *Mbio*, *12*, e02706–20.

Erdbrugger, U., Blijdorp, C. J., Bijnsdorp, I. V., Borras, F. E., Burger, D., Bussolati, B., Byrd, J. B., Clayton, A., Dear, J. W., Falcón-Pérez, J. M., Grange, C., Hill, A. F., Holthöfer, H., Hoorn, E. J., Jenster, G., Jimenez, C. R., Junker, K., Klein, J., Knepper, M. A., … Martens-Uzunova, E. S. (2021). Urinary extracellular vesicles: A position paper by the Urine Task Force of the International Society for Extracellular Vesicles. *Journal of Extracellular Vesicles*, *10*, e12093.

Gallemit, P. E. M., Yoodee, S., Malaitad, T., & Thongboonkerd, V. (2021). Epigallocatechin-3-gallate plays more predominant roles than caffeine for inducing actin-crosslinking, ubiquitin/proteasome activity and glycolysis, and suppressing angiogenesis features of human endothelial cells. *Biomedicine & Pharmacotherapy*, *141*, 111837.

Gilmore, W. J., Johnston, E. L., Zavan, L., & Bitto, N. J. (2021). Kaparakis-Liaskos M. Immunomodulatory roles and novel applications of bacterial membrane vesicles. *Molecular Immunology*, *134*, 72–85.

Hagey, D. W., Kordes, M., Gorgens, A., Mowoe, M. O., Nordin, J. Z., Moro, C. F., Löhr, J. M., & Andaloussi, E. (2021). Extracellular vesicles are the primary source of blood-borne tumour-derived mutant KRAS DNA early in pancreatic cancer. *Journal of Extracellular Vesicles*, *10*, e12142.

Hazrati, A., Malekpour, K., Soudi, S., & Hashemi, S. M. (2022). Mesenchymal stromal/stem cells spheroid culture effect on the therapeutic efficacy of these cells and their exosomes: A new strategy to overcome cell therapy limitations. *Biomedicine & Pharmacotherapy*, *152*, 113211.

Hong, J., Dauros-Singorenko, P., Whitcombe, A., Payne, L., Blenkiron, C., & Phillips, A. (2019). Analysis of the Escherichia coli extracellular vesicle proteome identifies markers of purity and culture conditions. *Journal of Extracellular Vesicles*, *8*, 1632099.

Hu, R., Li, J., Zhao, Y., Lin, H., Liang, L., Wang, M., Liu, H., Min, Y., Gao, Y., & Yang, M. (2020). Exploiting bacterial outer membrane vesicles as a cross-protective vaccine candidate against avian pathogenic *Escherichia coli* (APEC). *Microbial Cell Factories*, *19*, 119.

Hu, R., Lin, H., Wang, M., Zhao, Y., Liu, H., Min, Y., Yang, X., Gao, Y., & Yang, M. (2021). Lactobacillus reuteri-derived extracellular vesicles maintain intestinal immune homeostasis against lipopolysaccharide-induced inflammatory responses in broilers. *Journal of Animal Science and Biotechnology*, *12*, 25.

Jarry, A., Bossard, C., Bou-Hanna, C., Masson, D., Espaze, E., Denis, M. G., & Laboisse, C. L. (2008). Mucosal IL-10 and TGF-beta play crucial roles in preventing LPS-driven, IFN-gamma-mediated epithelial damage in human colon explants. *Journal of Clinical Investigation*, *118*, 1132–1142.

Jeppesen, D. K., Fenix, A. M., Franklin, J. L., Higginbotham, J. N., Zhang, Q., Zimmerman, L. J., Liebler, D. C., Ping, J., Liu, Q., Evans, R., Fissell, W. H., Patton, J. G., Rome, L. H., Burnette, D. T., & Coffey, R. J. (2019). Reassessment of exosome composition. *Cell*, *177*, 428–445. e18.

Kalluri, R., & LeBleu, V. S. (2020). The biology, function, and biomedical applications of exosomes. *Science*, 367.

Kanlaya, R., Naruepantawart, O., & Thongboonkerd, V. (2019). Flagellum is responsible for promoting effects of viable *Escherichia coli* on calcium oxalate crystallization, crystal growth, and crystal aggregation. *Frontiers in Microbiology*, *10*, 2507.

Kerr, N., Garcia-Contreras, M., Abbassi, S., Mejias, N. H., Desousa, B. R., Ricordi, C., Dietrich, W. D., Keane, R. W., & de Rivero Vaccari, J. P. (2018). Inflammasome proteins in serum and serum-derived extracellular vesicles as biomarkers of stroke. *Frontiers in Molecular Neuroscience*, *11*, 309.

Kranz, J., Schmidt, S., Lebert, C., Schneidewind, L., Mandraka, F., Kunze, M., Helbig, S., Vahlensieck, W., Naber, K., Schmiemann, G., & Wagenlehner, F. M. (2018). The 2017 update of the german clinical guideline on epidemiology, diagnostics, therapy, prevention, and management of uncomplicated urinary tract infections in adult patients: Part 1. *Urologia Internationalis*, *100*, 263–270.

Kumar, A., Dhadi, S. R., Mai, N. N., Taylor, C., Roy, J. W., Barnett, D. A., Lewis, S. M., Ghosh, A., & Ouellette, R. J. (2021). The polysaccharide chitosan facilitates the isolation of small extracellular vesicles from multiple biofluids. *Journal of Extracellular Vesicles*, *10*, e12138.

Lai, J., Wu, H., & Qin, A. (2021). Cytokines in febrile diseases. *Journal of Interferon & Cytokine Research*, *41*, 1–11.

Lamubol, J., Ohto, N., Kuwahara, H., & Mizuno, M. (2021). Lactiplantibacillus plantarum 22A-3-induced TGF-beta1 secretion from intestinal epithelial cells stimulated CD103(+) DC and Foxp3(+) Treg differentiation and amelioration of colitis in mice. *Food Function*, *12*, 8044–55.

Lee, H., Groot, M., Pinilla-Vera, M., Fredenburgh, L. E., & Jin, Y. (2019). Identification of miRNA-rich vesicles in bronchoalveolar lavage fluid: Insights into the function and heterogeneity of extracellular vesicles. *Journal of Controlled Release*, *294*, 43–52.

Li, J., Cai, S., Zeng, C., Chen, L., Zhao, C., Huang, Y., & Cai, W. (2022). Urinary exosomal vitronectin predicts vesicoureteral reflux in patients with neurogenic bladders and spinal cord injuries. *Experimental and Therapeutic Medicine*, *23*, 65.

Lian, Q., Xu, J., Yan, S., Huang, M., Ding, H., Sun, X., Bi, A., Ding, J., Sun, B., & Geng, M. (2017). Chemotherapy-induced intestinal inflammatory responses are mediated by exosome secretion of double-strand DNA via AIM2 inflammasome activation. *Cell Research*, *27*, 784–800.

Liu, D., Cao, S., Zhou, Y., & Xiong, Y. (2019). Recent advances in endotoxin tolerance. *Journal of Cellular Biochemistry*, *120*, 56–70.

Liu, F., Zhang, N., Wu, Y., Jiang, P., Jiang, T., Wang, Y., Zhang, Y., Zhai, Q., Zou, Y., & Feng, N. (2020). The pelvis urinary microbiome in patients with kidney stones and clinical associations. *BMC Microbiology*, *20*, 336.

Liu, Q., Yi, J., Liang, K., Zhang, X., & Liu, Q. (2017). Salmonella Choleraesuis outer membrane vesicles: Proteomics and immunogenicity. *Journal of Basic Microbiology*, *57*, 852–61.

Ma, M., Luo, Q., Fan, L., Li, W., Li, Q., Meng, Y., Yun, C., Wu, H., Lu, Y., Cui, S., Liu, F., Hu, B., Guan, B., Liu, H., Huang, S., Liang, W., Morgera, S., Krämer, B., Luan, S., … Yin, L. (2022). The urinary exosomes derived from premature infants attenuate cisplatin-induced acute kidney injury in mice via microRNA-30a-5p/mitogen-activated protein kinase 8 (MAPK8). *Bioengineered*, *13*, 1650–65.

Neugent, M. L., Hulyalkar, N. V., Nguyen, V. H., Zimmern, P. E., & De Nisco, N. J. (2020). Advances in understanding the human urinary microbiome and its potential role in urinary tract infection. *Mbio*, *11*, e00218–e00220.

Noonin, C., Kapincharanon, C., Sueksakit, K., Kanlaya, R., & Thongboonkerd, V. (2021). Application of tandem fast protein liquid chromatography to purify intact native monomeric/aggregated Tamm-Horsfall protein from human urine and systematic comparisons with diatomaceous earth adsorption and salt precipitation: yield, purity and time-consumption. *Analytical Methods*, *13*, 3359–3367.

Noonin, C., Peerapen, P., Yoodee, S., Kapincharanon, C., Kanlaya, R., & Thongboonkerd, V. (2022). Systematic analysis of modulating activities of native human urinary Tamm-Horsfall protein on calcium oxalate crystallization, growth, aggregation, crystal-cell adhesion and invasion through extracellular matrix. *Chemico-Biological Interactions*, *357*, 109879.

Noonin, C., & Thongboonkerd, V. (2021). Exosome-inflammasome crosstalk and their roles in inflammatory responses. *Theranostics*, *11*, 4436–51.

Pan, S., Zhang, Y., Huang, M., Deng, Z., Zhang, A., Pei, L., Wang, L., Zhao, W., Ma, L., Zhang, Q., & Cui, D. (2021). Urinary exosomes-based engineered nanovectors for homologously targeted chemo-chemodynamic prostate cancer therapy via abrogating EGFR/AKT/NF-kB/IkB signaling. *Biomaterials*, *275*, 120946.

Park, J. H. (2022). Regulation of in vivo fate of exosomes for therapeutic applications: New frontier in nanomedicines. *Journal of Controlled Release*, *348*, 483–8.

Peerapen, P., & Thongboonkerd, V. (2019). Protective cellular mechanism of estrogen against kidney stone formation: A proteomics approach and functional validation. *Proteomics*, *19*, e1900095.

Peerapen, P., & Thongboonkerd, V. (2020). Differential bound proteins and adhesive capabilities of calcium oxalate monohydrate crystals with various sizes. *International Journal of Biological Macromolecules*, *163*, 2210–2223.

Pongsakul, N., Vinaiphat, A., Chanchaem, P., Fong-ngern, K., & Thongboonkerd, V. (2016). Lamin A/C in renal tubular cells is important for tissue repair, cell proliferation, and calcium oxalate crystal adhesion, and is associated with potential crystal receptors. *Faseb Journal*, *30*, 3368–77.

Schroder, M., Meisel, C., Buhl, K., Profanter, N., Sievert, N., Volk, H. D., & Grütz, G. (2003). Different modes of IL-10 and TGF-beta to inhibit cytokine-dependent IFN-gamma production: consequences for reversal of lipopolysaccharide desensitization. *Journal of Immunology*, *170*, 5260–5277.

Shaw, G., Morse, S., Ararat, M., & Graham, F. L. (2002). Preferential transformation of human neuronal cells by human adenoviruses and the origin of HEK 293 cells. *Faseb Journal*, *16*, 869–871.

Singhto, N., Kanlaya, R., Nilnumkhum, A., & Thongboonkerd, V. (2018). Roles of macrophage exosomes in immune response to calcium oxalate monohydrate crystals. *Frontiers in Immunology*, *9*, 316.

Singhto, N., Sintiprungrat, K., & Thongboonkerd, V. (2013). Alterations in macrophage cellular proteome induced by calcium oxalate crystals: The association of HSP90 and F-actin is important for phagosome formation. *Journal of Proteome Research*, *12*, 3561–3572.

Singhto, N., & Thongboonkerd, V. (2018). Exosomes derived from calcium oxalate-exposed macrophages enhance IL-8 production from renal cells, neutrophil migration and crystal invasion through extracellular matrix. *Journal of Proteomics*, *185*, 64–76.

Sintiprungrat, K., Singhto, N., Sinchaikul, S., Chen, S. T., & Thongboonkerd, V. (2010). Alterations in cellular proteome and secretome upon differentiation from monocyte to macrophage by treatment with phorbol myristate acetate: insights into biological processes. *Journal of Proteomics*, *73*, 602–618.

Sutthimethakorn, S., & Thongboonkerd, V. (2020). Effects of high-dose uric acid on cellular proteome, intracellular ATP, tissue repairing capability and calcium oxalate crystal-binding capability of renal tubular cells: Implications to hyperuricosuria-induced kidney stone disease. *Chemico-Biological Interactions*, *331*, 109270.

Tan, Y. J., Wong, B. Y. X., Vaidyanathan, R., Sreejith, S., Chia, S. Y., Kandiah, N., & Ng, A. S. L. (2021). Altered cerebrospinal fluid exosomal microRNA levels in young-onset Alzheimer's disease and frontotemporal dementia. *Journal of Alzheimer's Disease Reports*, *5*, 805–813.

Tao, L., Zhou, J., Yuan, C., Zhang, L., Li, D., Si, D., Xiu, D., & Zhong, L. (2019). Metabolomics identifies serum and exosomes metabolite markers of pancreatic cancer. *Metabolomics*, *15*, 86.

Thongboonkerd, V., & Chaiyarit, S. (2022). Gel-based and gel-free phosphoproteomics to measure and characterize mitochondrial phosphoproteins. *Current Protocols*, *2*, e390.

Thongboonkerd, V., & Saetun, P. (2007). Bacterial overgrowth affects urinary proteome analysis: Recommendation for centrifugation, temperature, duration, and the use of preservatives during sample collection. *Journal of Proteome Research*, *6*, 4173–4181.

Tian, T., Han, J., Huang, J., Li, S., & Pang, H. (2021). Hypoxia-induced intracellular and extracellular heat shock protein gp96 increases paclitaxel-resistance and facilitates immune evasion in breast cancer. *Frontiers in Oncology*, *11*, 784777.

Tulkens, J., De Wever, O., & Hendrix, A. (2020). Analyzing bacterial extracellular vesicles in human body fluids by orthogonal biophysical separation and biochemical characterization. *Nature Protocols*, *15*, 4067.

Ugarte, F., Santapau, D., Gallardo, V., Garfias, C., Yizmeyian, A., Villanueva, S., Sepúlveda, C., Rocco, J., Pasten, C., Urquidi, C., Cavada, G., Martin, P. S., Cano, F., & Irarrázabal, C. E. (2021). Urinary extracellular vesicles as a source of NGAL for diabetic kidney disease evaluation in children and adolescents with type 1 diabetes mellitus. *Front Endocrinol (Lausanne)*, *12*, 654269.

Vergadi, E., Vaporidi, K., & Tsatsanis, C. (2018). Regulation of endotoxin tolerance and compensatory anti-inflammatory response syndrome by non-coding RNAs. *Frontiers in Immunology*, *9*, 2705.

Vitorino, R., Ferreira, R., Guedes, S., Amado, F., & Thongboonkerd, V. (2021). What can urinary exosomes tell us? *Cellular and Molecular Life Sciences*, *78*, 3265–3283.

Waller, T., Kesper, L., Hirschfeld, J., Dommisch, H., Kolpin, J., Oldenburg, J., Uebele, J., Hoerauf, A., Deschner, J., Jepsen, S., & Bekeredjian-Ding, I. (2016). Porphyromonas gingivalis outer membrane vesicles induce selective tumor necrosis factor tolerance in a toll-like receptor 4- and mTOR-dependent manner. *Infection and Immunity*, *84*, 1194–1204.

Wang, C., Liu, X., Li, H., Zhao, L., Kong, G., Chen, J., Li, Z., Qi, J., Tian, Y., & Zhang, F. (2022). Urinary exosome-based androgen receptor-variant 7 detection in metastatic castration-resistant prostate cancer patients. *Translational Andrology and Urology*, *11*, 202–212.

Weingrill, R. B., Paladino, S. L., Souza, M. L. R., Pereira, E. M., Marques, A. L. X., Silva, E. C. O., da Silva Fonseca, E. J., Ursulino, J. S., Aquino, T. M., Bevilacqua, E., Urschitz, J., Silva, J. C., & Borbely, A. U. (2021). Exosome-enriched plasma analysis as a tool for the early detection of hypertensive gestations. *Frontiers in Physiology*, *12*, 767112.

Yoodee, S., Noonin, C., Sueksakit, K., Kanlaya, R., Chaiyarit, S., Peerapen, P., & Thongboonkerdet, V. (2021). Effects of secretome derived from macrophages exposed to calcium oxalate crystals on renal fibroblast activation. *Communications Biology*, *4*, 959.

Yoodee, S., Peerapen, P., Plumworasawat, S., & Thongboonkerd, V. (2021). ARID1A knockdown in human endothelial cells directly induces angiogenesis by regulating angiopoietin-2 secretion and endothelial cell activity. *International Journal of Biological Macromolecules*, *180*, 1–13.

Zhang, L., Qu, L., Zhang, Y., Xu, Z., & Tang, H. (2022). Differential expression of circular RNAs in plasma exosomes from patients with ankylosing spondylitis. *Cell Biology International*, *46*, 649–659.

Zhao, F., Zheng, T., Gong, W., Wu, J., Xie, H., Li, W., Zhang, R., Liu, P., Liu, J., Wu, X., Zhao, Y., & Ren, J. (2021). Extracellular vesicles package dsDNA to aggravate Crohn's disease by activating the STING pathway. *Cell Death & Disease*, *12*, 815.

Zhu, Q., Huang, L., Yang, Q., Ao, Z., Yang, R., Krzesniak, J., Lou, D., Hu, L., Dai, X., Guo, F., & Liu, F. (2021). Metabolomic analysis of exosomal-markers in esophageal squamous cell carcinoma. *Nanoscale*, *13*, 16457–16464.

Zwarycz, A. S., Livingstone, P. G., & Whitworth, D. E. (2020). Within-species variation in OMV cargo proteins: The Myxococcus xanthus OMV pan-proteome. *Molecular Omic*, *16*, 387–397.

SUPPORTING INFORMATION

Additional supporting information can be found online in the Supporting Information section at the end of this article.

How to cite this article: Noonin, C., Peerapen, P., & Thongboonkerd, V. (2022). Contamination of bacterial extracellular vesicles (bEVs) in human urinary extracellular vesicles (uEVs) samples and their effects on uEVs study. *Journal of Extracellular Biology*, *1,* e69. https://doi.org/10.1002/jex2.69